Stability of a Sn_4 tetrahedral cluster in an alkali atom environment

Bing Wang and M. J. Stott
Department of Physics, Queen's University, Kingston, Ontario K7L 3N6, Canada

J. A. Alonso
Departamento de Física Teórica, Universidad de Valladolid, Valladolid 47011, Spain
(Received 22 July 2001; published 2 January 2002)

The stability of a Sn_4 tetrahedral cluster in an alkali atom environment is studied by calculations on a series of A_nSn_4 (A=Li, Na, and K) clusters, in which, starting at $n=4$, alkali atoms are added one by one until $n=10$. The results show that the Sn_4 tetrahedron is unstable in Li_nSn_4 clusters, opening into a Sn_4 butterfly at $n=5$, and completely broken at $n=10$. For K_nSn_4 clusters, however, the Sn_4 tetrahedron remains robust for all values of n, while Na_nSn_4 clusters are an intermediate case in which the Sn_4 tetrahedron opens into a butterfly at $n=8$. The size of the alkali atoms and the strength of the bonding between them determine whether the Sn_4 tetrahedron breaks up or not, and the Li_2 unit is found to be responsible for cutting the Sn-Sn bonds of the Sn_4 tetrahedron in Li_nSn_4 clusters. The results are discussed in relation to the corresponding alkali-tin bulk alloys.

DOI: 10.1103/PhysRevB.65.045410 PACS number(s): 61.46.+w, 36.40.Cg, 36.40.Mr, 36.40.Qv

I. INTRODUCTION

There is an increasing interest in the relationship between the stability of some bulk materials and the properties of small gas-phase clusters that could form building blocks of those bulk materials.[1] Studies of such a relationship will provide useful clues for developing cluster-assembled materials with expected properties. The prototypical case is a solid fullerite composed of C_{60} molecules,[2] and computer simulations that explored the synthesis of materials by the self-assembling of doped aluminum clusters.[3] There are, however, some binary compounds which may be viewed as naturally occurring cluster-assembled materials.[1] An example of such intermetallic compounds, which was studied extensively in recent years,[4–9] is the family of alkali-group IV alloys, whose structures and properties also appear to be related to small gas-phase clusters.

The phase diagrams of solid alkali-tin alloys[10] indicate that, for a Li-Sn system, stable compounds concentrate around the octet composition Li_4Sn, while for a Na-Sn system a number of stable compounds are found at both Na-rich (near the octet composition) and Sn-rich compositions. For the K-Sn system, the equiatomic compound is very stable with a melting temperature of 830 °C (compared with melting temperatures of 578 °C for the equiatomic NaSn compound and 486 °C for the equiatomic LiSn compound); and there is only one K-rich compound (K_2Sn) and there are two Sn-rich compounds. A related trend was observed in some properties of liquid alloys.[4] For example, the electrical resistivity of a liquid Li-Sn alloys exhibits a high peak around 20% Sn. For liquid K-Sn alloys the peak is shifted to 50% Sn, while liquid Na-Sn alloys comprise an intermediate case with peaks at both 20% Sn and 50% Sn.[11] Those peaks again highlight the octet and equiatomic compositions. It is therefore tempting to speculate that features at these stoichiometries are related to the stability of some particular gas-phase clusters. Plausible candidate clusters are A_4M corresponding to the octet composition, and A_4M_4 corresponding to the equiatomic composition, where A stands for an alkali element and M represents a group-IV element. Calculations have shown that free A_4M and A_4M_4 clusters are particularly stable.[12,13] The structure of the A_4M_4 clusters consists of an inner tetrahedron of M atoms surrounded by A atoms forming an opposed tetrahedron. Such M_4 tetrahedra exist in the solid compounds of 50% Pb (or Si, Ge, Sn) with Na and heavier alkalis, which crystallize in a body-centered-tetragonal structure.[4,14] In this structure, all 32 Pb (or Si, Ge, Sn) atoms in the unit cell are arranged in the form of Pb_4 tetrahedra, while the Na atoms occupy the space between the tetrahedra. The corresponding solids of M with Li, however, do not follow this pattern. Although calculations indicate that free Li_4M_4 clusters are rather stable and form the same M_4 tetrahedra,[12,13] these are not present in the equiatomic LiM solid, which instead crystallizes in a CsCl structure in which each M atom has eight Li atoms as nearest neighbors.

A simple model proposed by Zintl and co-workers[15] accounts for the appearance of tetrahedral units in alloys of 50% M with alkalis other than Li. According to this model, the stability of M_4 tetrahedra is owed to the transfer of one electron from each alkali atom to an M atom. The M^- anions are isoelectronic to P atoms, and so tend to form tetrahedral arrangements like those of typical tetrahedral P_4 molecules. The structural trend in the solid alloys from Li to the heavy alkalis was explained by Geertsma and co-workers[4,16] as a combined effect of the Zintl concept and the increasing size of the alkali cations, whose role is mainly to separate the $(M_4)^{4-}$ anions. For equiatomic liquid alkali-tin and lead alloys, the first sharp diffraction peaks in neutron-diffraction experiments were interpreted as an indication of the existence of M_4 (M=Sn, Pb) tetrahedra in the alloys.[4,14] However, *ab initio* molecular-dynamics simulations found M_4 tetrahedra only in liquid alloys with K while in LiM and NaM alloys a connected network of isolated M atoms forms instead.[5,6,9] Nevertheless, it should be noted that the conclusions from *ab initio* molecular-dynamics simulations are restricted by the system size and simulation times. On the other hand, the structural features of alkali-tin and alkali-lead solid alloys agree with the explanations in Refs. 4 and 16, which is

confirmed by *ab initio* molecular-dynamics simulations.[9] For alkali-lead solid alloys, the stability of the Pb_4 tetrahedra was also studied by *ab initio* simulations of the assembling of these intermetallic compounds from the corresponding A_4Pb_4 clusters.[8] The results are also consistent with the explanations of Refs. 4 and 16. As the clusters are brought together to form a solid, the inner Pb_4 units proved to be remarkably robust and insensitive to the change in the alkali environment for the cases of Na and heavier alkalis. The alkali atoms merely serve as cheap sources of electrons to be transferred to the Pb_4 units, and for separating the tetrahedra. In the case of LiPb alloys, the Li ions are too small to properly separate the Pb_4 tetrahedra, and so the CsCl structure is more stable than a clustered structure. The relation between the atomic size effect and the stability of the tetrahedral complexes in solid and liquid alkali-lead alloys was also addressed in our early work.[13]

If the sizes of the alkali atoms, or in other words, the separation of the tetrahedra by the alkali atoms, were the only factor determining the stability of the clustered structure; thus we would expect to find tetrahedra in alkali-rich solid alloys because the tetrahedra would be even further separated. However, there seems to be no evidence of such features. We might also expect to find group-IV tetrahedra in alkali-rich liquid alloys for the same reason, but none has been detected. Obviously there are other effects which could affect the stability of the tetrahedra in alkali-rich alloys. Here we report an investigation of these effects.

Rather than studying the stability of the tetrahedra by performing molecular-dynamics simulations directly on alkali-rich AM alloys, which would be very time consuming, we have performed simulations on small clusters, which, we believe, can provide some important physical insight from a different point of view. Sn is the group-IV element we shall focus on, but clusters of alkalis with Ge and particularly Pb should be very similar to systems involving Sn. We have started from an A_4Sn_4 cluster, which is particularly stable, and added A atoms to the cluster one by one. The purpose of this work is to see whether the Sn_4 tetrahedron breaks up as more alkali atoms are added. *Ab initio* plane-wave pseudopotential methods[17] have been used to relax the atomic arrangement and find the equilibrium structure. The calculations give the equilibrium arrangement of the four Sn atoms as they are clad with increasing amounts of the alkali. The results for $A=$Li, Na, and K reveal a trend in the stability of the Sn_4 tetrahedron with the choice of alkali, which is consistent with Refs. 4 and 16 and the experimental trends displayed in the phase diagrams and by electrical resistivity measurements.

The calculational method is described briefly in Sec. II. The presentation of the results and the discussion of their significance then follow, and Sec. IV gives concluding remarks.

II. COMPUTATIONAL DETAILS

The calculations were performed using the computer code developed by Scheffler and co-workers[17] The local density approximation to the exchange and correlation energies[18] was applied, using the Perdew-Zunger parametrization[19] of the electron gas results of Ceperley and Alder.[20] Norm-conserving, spin-averaged scalar relativistic pseudopotentials[21] with the Kleinman-Bylander separable form[22] were generated for Sn, Li, Na, and K. For alkalis, a nonlinear core correction[23] was incorporated into the exchange-correlation potential. The pseudopotentials were first tested on the corresponding dimers and bulk metals. The bond lengths of the dimers and the lattice constants of the metals were predicted within 5% of the experimental values. The calculations for alkali-tin clusters were performed in a simple cubic supercell of lattice constant 34 a.u., and a single $\mathbf{k}$ point (Γ) was used for the sampling of the Brillouin zone. Energies well converged to 0.001 Hartree were obtained with a plane-wave energy cutoff of 8 Ry. Although spin-polarization effects were not included, calculations for Na_nSn ($n=3-8$) clusters show that spin-polarization does not significantly alter the trends in the structures, binding energies, and bond lengths of these clusters.[24]

Starting from the highly symmetrical A_4Sn_4 cluster, alkali atoms were added one by one until the number of alkali atoms in the cluster was ten. Since the stability of the Sn_4 tetrahedron is of interest, the geometry optimizations were started with initial configurations in which the alkali atoms are capping faces or edges of the Sn_4 tetrahedron. For the clusters with less than ten alkali atoms, there are a number of likely locations for the added alkali atom, and all of them were used as initial configurations. In the cases with ten alkali atoms, the prescription gives only one possibility for alkali atoms around the Sn_4 tetrahedron, with all four faces and six edges of the tetrahedron capped by an alkali atom, respectively. Since in such an atomic arrangement the Sn_4 tetrahedron may not break up just because of the high symmetry of the structure, we also considered some initial configurations other than Sn_4 tetrahedral symmetry for $A_{10}Sn_4$ clusters. All the initial structures considered were relaxed to the energy minimum using damped Newtonian dynamics,[17] which started with small damping and used increasing damping as the equilibrium was approached.

III. RESULTS AND DISCUSSION

In Figs. 1 and 2, we show the lowest-energy structure we found from the initial configurations described above for each of A_nSn_4 ($n=5-10$) clusters. The A_4Sn_4 clusters have the same lowest-energy structure for $A=$Li, Na, and K, which consists of a Sn_4 tetrahedron sitting inside an opposed A_4 tetrahedron. This symmetric structure is very stable. The Sn-Sn bond length is about 3.03 Å and the dihedral angle of the Sn_4 tetrahedron is about 70°. Starting from $n=5$, the lowest energy structure of the A_nSn_4 cluster shows differences between $A=$Li and $A=$Na, K. For Li_5Sn_4, one bond of the Sn_4 tetrahedron breaks, and the tetrahedron opens into a butterfly with a dihedral angle of 97° between the two wings and a distance of 3.84 Å between the two Sn atoms with a broken bond. In contrast, the Sn_4 tetrahedron remains stable in Na_5Sn_4 and K_5Sn_4, although it is slightly distorted for Na_5Sn_4. For Na_5Sn_4, an isomer with a structure similar to the lowest-energy structure of K_5Sn_4 (four alkali atoms cap-

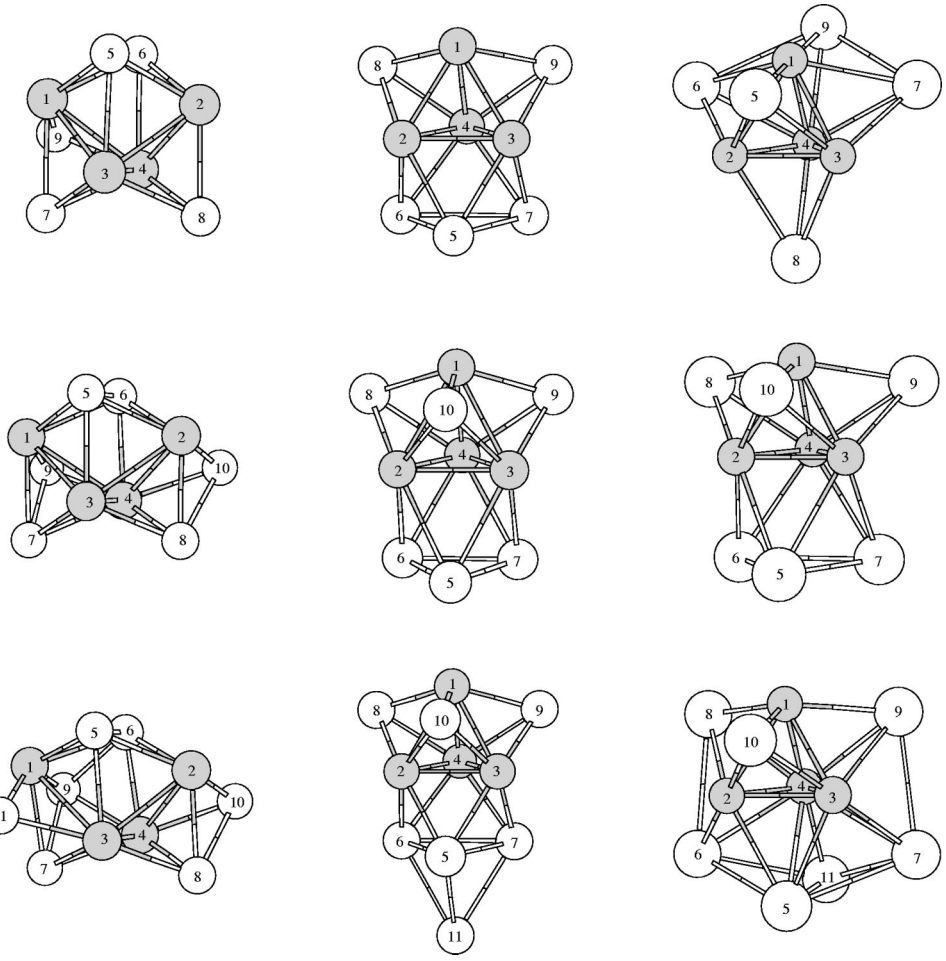

FIG. 1. From the left to right panels: the lowest-energy structures of Li_nSn_4, Na_nSn_4, and K_nSn_4 ($n=5-7$) clusters. A filled sphere is an alkali atom, and an empty sphere is a Sn atom. Atoms are assigned numbers for identification.

ping the faces and one atom capping an edge of the tetrahedron) was found to be a local minimum with energy just 0.04 eV above the ground state. Thus for $n=5$ there is no significant difference between Na and K clusters. In Li_6Sn_4, the Sn_4 butterfly opens further with the dihedral angle increased to 104°, and the corresponding broken-bond length increased to 4.18 Å. On the other hand, the Sn_4 tetrahedron remains in Na_6Sn_4 and K_6Sn_4, which have similar lowest-energy structures.

At $n=7$, the Sn_4 butterfly no longer exists in Li_7Sn_4, since two Sn-Sn bonds have been broken. The lowest-energy structures of Na_7Sn_4 and K_7Sn_4 are now substantially different, although both result from the relaxation of the same initial configuration. Moreover, for Na_7Sn_4, there is a local minimum with almost the same energy as the ground state (only 0.02 eV higher), where the Sn_4 tetrahedron breaks up into a butterfly with a dihedral angle of 101° between the two wings and a distance of 4.12 Å between the two Sn atoms of the broken bond. It seems that $n=7$ is a transitional stage for Na_nSn_4 clusters, at which a substantial distortion of the Sn_4 tetrahedron develops. However, for K_7Sn_4, no local minimum has been found in which the Sn_4 tetrahedron opens into a butterfly.

In the lowest-energy structure of Li_8Sn_4, the Sn_4 tetrahedron has broken to such a degree that two Sn-Sn interatomic distances have increased above 4.0 Å [4.58 Å for the Sn(1)-Sn(2) distance and 4.20 Å for the Sn(1)-Sn(3) distance; cf. Fig. 2]. The Sn_4 tetrahedron finally opens up into a butterfly for Na_8Sn_4, while K_8Sn_4 has an atomic arrangement rather similar to that of Na_8Sn_4 but with all the Sn-Sn bonds intact. In Li_9Sn_4, three Sn atoms, Sn(1), Sn(2), and Sn(3), which were initially on one face of the tetrahedron, are dispersed with the Sn-Sn distances all above 4.1 Å. In Na_9Sn_4, the Sn_4 butterfly opens further with a dihedral angle of 105° between the two wings and a distance of 4.38 Å between the two Sn atoms of the broken bond. However, the Sn_4 tetrahedron persists in K_9Sn_4 without appreciable distortion.

In the case of $n=10$, we first considered an initial configuration containing the Sn_4 tetrahedron with all the four faces and six edges capped by alkali atoms. For $Li_{10}Sn_4$, this initial configuration evolves into a distorted cube formed by four Sn atoms and four Li atoms, with the other six Li atoms capping the six faces of the cube. At this stage the Sn_4 tetrahedron is completely broken apart with the Sn-Sn interatomic distances of 3.72 Å. For $Na_{10}Sn_4$ and $K_{10}Sn_4$, the Sn_4 tetrahedron remains in a relaxed structure, which has the same atomic arrangement as the initial configuration with small changes in bond lengths. This occurs presumably because of the high symmetry of the starting configuration. To see if the Sn_4 tetrahedron is really stable with ten Na or K atoms, we considered another initial configuration with four Sn atoms arranged in the form of two Sn dimers surrounded by alkali atoms. This alternative arrangement was motivated

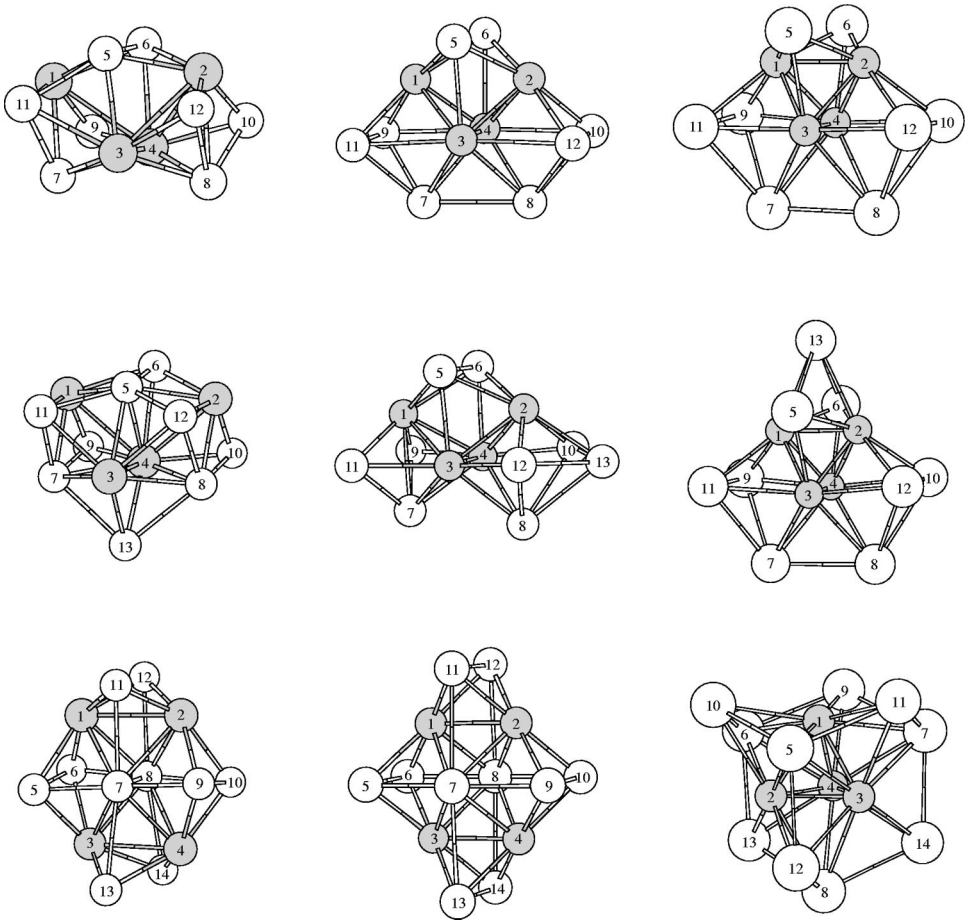

FIG. 2. From the left to right panels: the lowest-energy structures of Li_nSn_4, Na_nSn_4, and K_nSn_4 ($n=8-10$) clusters. A filled sphere is an alkali atom, and an empty sphere is a Sn atom. Atoms are assigned numbers for identification.

by *ab initio* molecular-dynamics simulations on the liquid alloy of 20% Sn with Na, which shows the existence of only isolated Sn atoms and Sn dimers.[5] The relaxed structure still contains two Sn dimers in a similar atomic arrangement. For $Li_{10}Sn_4$, it is about 0.75 eV lower in energy than the other isomer containing a distorted cube, and it is 1.1 eV lower in energy than the other isomer for $Na_{10}Sn_4$, while for $K_{10}Sn_4$ it is about 0.1 eV higher in energy. For $K_{10}Sn_4$ the four Sn atoms group together in a square with an edge of 3.02 Å while in $Na_{10}Sn_4$ and $Li_{10}Sn_4$ the distances between the two Sn dimers are 3.77 and 4.03 Å, respectively. In Fig. 2, we only show the lowest-energy isomers, i.e., the isomer containing two Sn dimers for $Li_{10}Sn_4$ and $Na_{10}Sn_4$, and the isomer with the Sn_4 tetrahedron for $K_{10}Sn_4$. We also studied the addition of 14 Na atoms around a Sn_4 tetrahedron, and found that the Sn_4 tetrahedron breaks up directly into two Sn dimers. Thus for Na_nSn_4 clusters the Sn_4 tetrahedron appears to break up into two Sn dimers at $n=10$. For $K_{10}Sn_4$, we relaxed another initial configuration similar to the first isomer of $Li_{10}Sn_4$ cluster, i.e., a distorted cube formed by four Sn atoms and four K atoms with the cube faces capped by the other six K atoms. Upon relaxation, the four Sn atoms group together in the form of a tetrahedron with the Sn-Sn interatomic distances of 2.99 Å, while the K atoms cap all the faces and edges, which is the same structure shown in Fig. 2 for $K_{10}Sn_4$. Clearly the Sn_4 tetrahedron is still very stable in the $K_{10}Sn_4$ cluster.

The lowest-energy structures of the Li_nSn_4 clusters, displayed in Figs. 1 and 2, show that the breakup of a Sn-Sn bond is accompanied by the formation of Li-Li bonds. For example, for $n=5-9$, bonding between Li(5) and Li(6) atoms breaks the bond between Sn(1) and Sn(2). In addition, in Li_7Sn_4, the Li(7)-Li(9) and Li(9)-Li(6) bonds break the Sn(1)-Sn(4) bond; in Li_8Sn_4 and in Li_9Sn_4, the Li(5)-Li(11) and Li(11)-Li(7) bonds break the Sn(1)-Sn(3) bond; and in Li_9Sn_4, the Li(5)-Li(12) and Li(12)-Li(8) bonds break the Sn(2)-Sn(3) bond. The Li-Li bond lengths in the newly formed bonds are close to and, in some cases, up to 4% smaller than the bond length (2.71 Å) of a free Li dimer obtained in a supercell calculation with the same energy cutoff and lattice parameter. As Li atoms are added to the Li_4Sn_4, the Li-Sn bond lengths decrease on the average, which suggests that the interaction between Li and Sn atoms becomes stronger. Also, for Na_nSn_4 clusters with $n=7-9$, the Na-Sn bond lengths decrease on the average. However, for Na_nSn_4 clusters with n up to 7 and for all K_nSn_4 clusters, the Na-Sn and K-Sn bond lengths increase as the number of Na or K atoms increases.

In recent work on the clustering behavior in bimetallic clusters of *sp* elements, Majumder *et al.*[25] found that differences in elemental parameters such as the atomic radius, number of valence electrons, and the binding energies of dimers are factors affecting the clustering behavior. Compared with Na and K, Li shows significant differences in those elemental properties, which are summarized in Table I. We have also listed the corresponding properties of Sn. A Li

TABLE I. Summary of the properties of Li, Na, K. and Sn. For alkalis, the solid refers to a bcc metal, and for Sn, to the diamond structure. Dimers were calculated by the supercell method, with the same parameters used for A_nSn_4 clusters. The calculations for solids employed 64 **k** points and an energy cutoff of 16 Ry.

	Li	Na	K	Sn
Ionic radius (Å)[a]	0.68	0.97	1.33	0.71
Dimer bond length (Å)				
Calculated	2.68	3.04	3.79	2.71
Experimental	2.67[b]	3.08[b]	3.90[b]	2.75[c]
Bond length in solid (Å)				
Calculated	2.90	3.51	4.37	2.80
Experimental[a]	3.02	3.66	4.52	2.81
Dimer binding energy (eV)	1.05[b]	0.72[b]	0.51[b]	1.91[d]
Cohesive energy of solid (eV/atom)[a]	1.63	1.11	0.93	3.14

[a]Reference 26.
[b]Reference 27.
[c]Reference 28.
[d]Reference 29.

ion is smaller than Na and K ions, and the Li atoms are more''sticky,'' having larger bonding energies. From Table I we see that, among the three alkalis, only Li can compete with Sn in both size and bonding strength. That Li atoms are more sticky is also reflected in the evaporation energy of an alkali-tin cluster, which is defined as the energy required for removing one alkali atom from the cluster. In Fig. 3, we plot the evaporation energies of A_nSn_4 $(n=5-10)$ clusters whose structures are shown in Figs. 1 and 2. The evaporation energies of Li_nSn_4 clusters are substantially larger (by a factor of 2) than those of corresponding Na_nSn_4 and K_nSn_4 clusters, a result consistent with the earlier calculations of A_nPb and A_nPb_4 $(n=1-5)$ clusters.[12,13]

From the discussion in the above paragraphs, we conclude that the small size of the Li atoms and the relatively strong Li-Li bond are the main factors leading to the breakup of the Sn_4 tetrahedron in Li_nSn_4 clusters. Because Li atoms are small, a bonded Li-Li pair can squeeze into a Sn_4 tetrahedron, breaking a Sn-Sn bond. As more Li atoms are added, more Li dimers squeeze into a Sn_4 tetrahedron and break more Sn-Sn bonds. Na atoms are larger and the Na-Na bond is weaker, so a Na-Na pair cannot squeeze so easily into the Sn_4 tetrahedron in a Na_nSn_4 cluster. In fact, the effect of the Na dimer breaking a Sn-Sn bond in Na_8Sn_4 and Na_9Sn_4 is less drastic than the corresponding effect of the Li dimers in Li_8Sn_4 and Li_9Sn_4. In Na_8Sn_4, the dihedral angle between the plane defined by the Sn(1), Na(5), and Na(6) atoms and the plane defined by the Sn(2), Na(5), and Na(6) atoms is 110°, while the corresponding dihedral angle in Li_8Sn_4 is 144°. In Li_9Sn_4, the Li(5), Li(6), Li(11), and Li(12) atoms have invaded the Sn_4 tetrahedron and broken up the triangle formed by the Sn(1), Sn(2), and Sn(3) atoms, while in Na_9Sn_4, the Na pair leading to the breakup of the Sn-Sn bond is still above the Sn_4 butterfly. Since the Na dimer cannot squeeze into the Sn_4 tetrahedron, two Sn atoms cannot be separated to a distance comparable to that in the Li-Sn clusters. As for K_nSn_4 clusters, the K atoms are so large and the bonding between them is so weak that they never have a chance to distort a Sn_4 tetrahedron or, needless to say, to break a Sn-Sn bond. As more K atoms are added, they tend to stay further away from the Sn_4 tetrahedron, as indicated by the increase of the average K-Sn distances, in order to make room for more K atoms in the surrounding shell. The four extra electrons required for the establishment of the $(Sn_4)^{4-}$ polyanion are contributed by the whole K shell around the tetrahedron. In the case of a K_4Sn_4 cluster, each of the four K atoms contributes one electron to the $(Sn_4)^{4-}$ polyanion, and so the electrostatic interaction between K and Sn atoms is stronger and the K atoms are drawn closer to the Sn_4 tetrahedron.

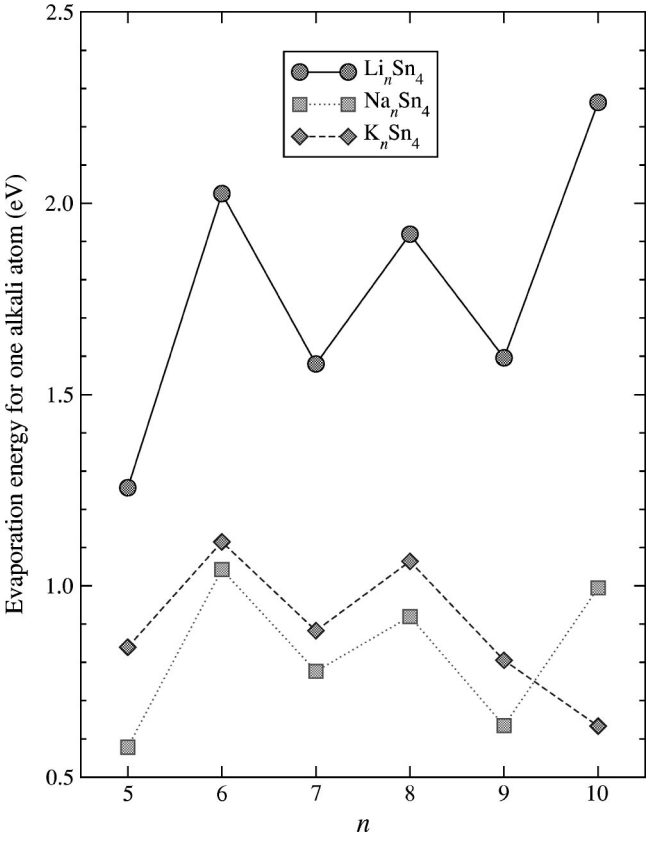

FIG. 3. Evaporation energies for removing one alkali atom from A_nSn_4 (A=Li, Na, and K, and $n=5-10$) clusters whose structures are shown in Figs. 1 and 2.

To further our understanding on the stability of the Sn_4 tetrahedron, we plot diagrams of Kohn-Sham (KS) energy levels in Figs. 4–6 for the clusters shown in Figs. 1 and 2. The highest occupied molecular orbital (HOMO) of each cluster is marked by a right-pointing arrow, and level degeneracies are indicated explicitly. We also plot the KS levels for a pure Sn_4 tetrahedral isomer and for single alkali and Sn atoms, all of which were calculated using the same method and parameters as for A_nSn_4 clusters.

The outer electronic structure of the Sn atom is $5s^25p^2$. The energy levels of the A_nSn_4 clusters in Figs. 4–6 are clearly separated into two groups. The deeply bound states in the range from -12.5 to -7.5 eV are molecular orbitals originating predominantly from Sn $5s$ levels. Above these,

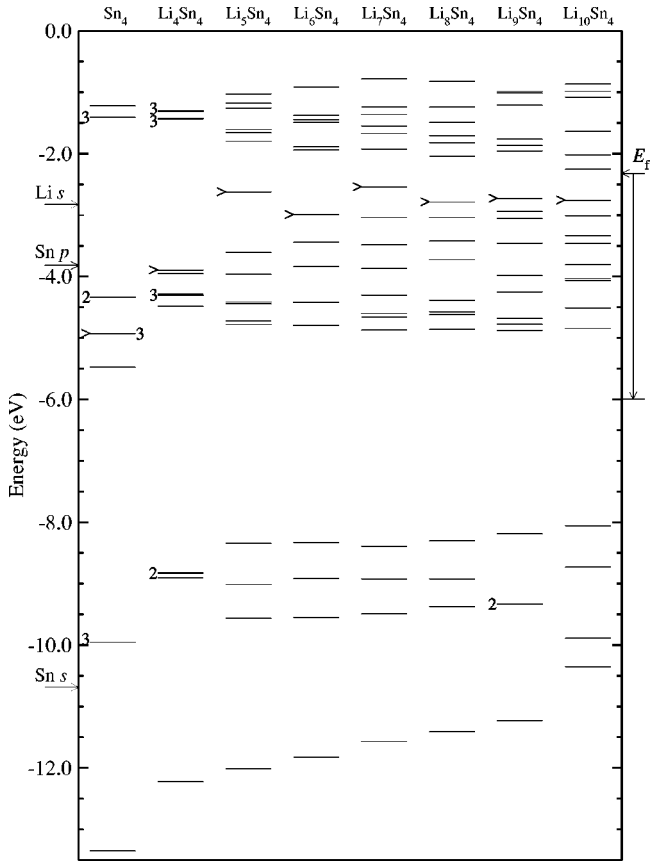

FIG. 4. The KS energy levels of a Sn_4 tetrahedron and the Li_nSn_4 ($n=4-10$) clusters whose structures are shown in Figs. 1 and 2. The HOMO's are marked by right-pointing arrows, and the number beside an energy level represents the degeneracy. The KS energy levels of single Li and Sn atoms are indicated on the left side of the figure. The Fermi energy E_f and the conduction bandwidth of a Li bcc metal are shown on the right side of the figure.

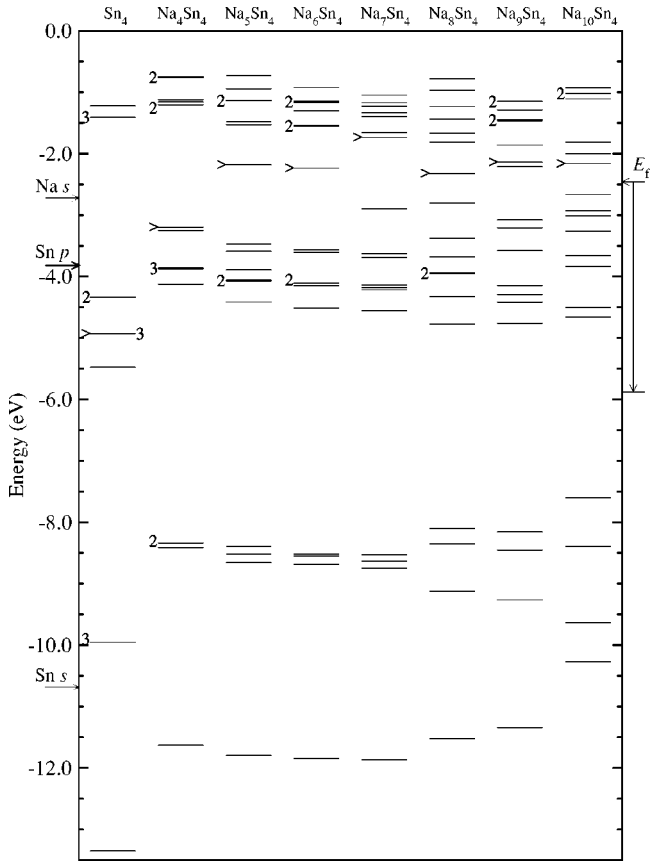

FIG. 5. The KS energy levels of a Sn_4 tetrahedron and the Na_nSn_4 ($n=4-10$) clusters whose structures are shown in Figs. 1 and 2. The HOMO's are marked by right-pointing arrows, and the number beside an energy level represents the degeneracy. The KS energy levels of single Na and Sn atoms are indicated on the left side of the figure. The Fermi energy E_f and the conduction bandwidth of a Na bcc metal are shown on the right side of the figure.

and separated from them by a gap larger than 3.0 eV, there is a band of molecular orbitals formed by Sn $5p$ orbitals mixed with the alkali s orbitals, which will be discussed in detail later. The ground-state structure of Sn_4, with 16 valence electrons, is a planar rhombus,[30] but this cluster has a low-lying tetrahedral isomer. As shown in Figs. 4–6, the energy levels of this tetrahedral isomer display a pattern of degeneracies 1:3:1:3:2 with the doubly degenerate lowest unoccupied molecular orbital (LUMO) and a large gap of 2.9 eV between the LUMO and the next unoccupied level. Filling of this doubly degenerate LUMO, which requires four extra electrons, will make the tetrahedral cluster a very stable closed-shell species with a substantial HOMO-LUMO gap.[13] In Li_4Sn_4 this gap amounts to 2.5 eV. When alkali atoms are added to the Sn_4 unit, the key to the stability of a tetrahedral structure is the complete electron transfer from the alkali atoms to Sn_4. Adding one alkali atom to Sn_4 obviously will not stabilize the Sn_4 tetrahedron. Our previous calculations[31] showed that, for $NaSn_4$, the lowest-energy structure is a slightly distorted Sn_4 rhombus with the Na atom sitting above it. But $NaSn_4$ has another isomer which can be viewed as a distorted Sn_4 tetrahedron with one face capped by a Na atom. The energy difference between this isomer and the one with a Sn_4 rhombus is just 0.07 eV, to be contrasted with 1.2 eV for the pure Sn_4 cluster. The lowest-energy structure of Na_2Sn_4 clearly indicates a somewhat distorted Sn_4 tetrahedron with Na atoms capping two of the faces. This structure is now about 0.6 eV lower in energy than the other isomer of Na_2Sn_4 which contains a Sn_4 rhombus with a Na atom sitting on each side. The effect of adding alkali atoms is similar to that of adding extra electrons to a neutral Sn_4 cluster;[30] however, in the former case the charge transfer is facilitated by alkali atoms and completed for a closed shell when four alkali atoms are added to the well-separated sites above the four faces of the Sn_4 tetrahedron.

When a Li atom is added to Li_4Sn_4 to form Li_5Sn_4, this Li atom has to sit close to one of the other Li atoms. Evidently, the argument given up to this point applies also to the clusters with Na or K. But now a key ingredient enters the picture, which differentiates clusters with Li from those with Na or K: the binding energy of a Li dimer is substantially larger than that of Na or K dimers, and its bond length shorter, as shown in Table I. Thus in Li_5Sn_4 two Li atoms bind together. There is, nevertheless, substantial mixing between the mo-

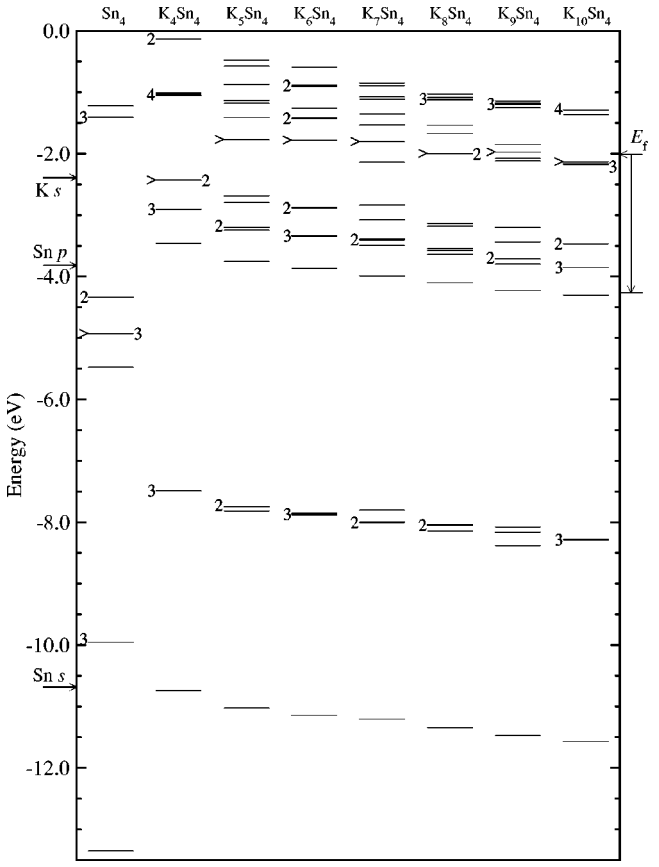

FIG. 6. The KS energy levels of a Sn_4 tetrahedron and the K_nSn_4 ($n=4-10$) clusters whose structures are shown in Figs. 1 and 2. The HOMO's are marked by right-pointing arrows, and the number beside an energy level represents the degeneracy. The KS energy levels of single K and Sn atoms are indicated on the left side of the figure. The Fermi energy E_f and the conduction bandwidth of a K bcc metal are shown on the right side of the figure.

lecular orbitals contributing to this alkali bond and the outer orbitals of the $(Sn_4)^{4-}$ polyanion. Due to this hybridization and the reduced cluster symmetry, the manifold of orbital states associated with the polyanion splits and broadens, as shown in Fig. 4. The separation between the singly occupied HOMO of Li_5Sn_4, which lies in the middle of the HOMO-LUMO gap of Li_4Sn_4, and the next occupied state is 1.0 eV, and this reduced separation indicates that Li_5Sn_4 cannot be interpreted as a closed-shell Li_4Sn_4 cluster with a Li atom attached. Instead, the formation of a Li-Li bond observed in Fig. 1, which acts as a blade cutting a Sn-Sn bond, is a better description (also note that the Li-Li and Sn-Sn bond lengths are similar). A complementary view of the process is that the charge transfer from the Li atoms to Sn_4 is reduced by the formation of the Li-Li bond and, as a consequence, the tetrahedron opens up into a butterfly. These effects become enhanced as more Li atoms are added to form Li_6Sn_4, Li_7Sn_4, etc. Figure 7 presents a contour plot of the electron density in a plane of Li_6Sn_4 through the newly formed Li-Li bond. The accumulation of charge in the region between two Li atoms is evident. From Li_6Sn_4 to $Li_{10}Sn_4$, a broad band of hybridized energy levels forms, and in $Li_{10}Sn_4$, the lower band with

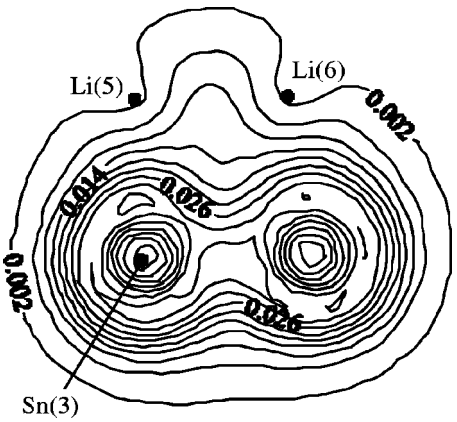

FIG. 7. Electron-density contour plot on the plane composed of atoms Sn(3), Li(5), and Li(6) of the Li_6Sn_4 cluster whose structure is shown in Fig. 1.

pure Sn *s* character is separated into two groups because of the two Sn dimers contained in the structure.

The evolution of the electronic structure in the Na clusters, shown in Fig. 5, is different. The HOMO-LUMO gap of Na_4Sn_4 is 2.0 eV. After adding one or two Na atoms to form Na_5Sn_4 or Na_6Sn_4, the newly occupied level lies in the region of the HOMO-LUMO gap of Na_4Sn_4, as for the corresponding Li clusters. However, the interaction between this level and the manifold of states of $(Sn_4)^{4-}$ is repulsive, and the closed-shell structure of the $(Sn_4)^{4-}$ polyanion turns out to be further stabilized by the presence of the fifth and sixth Na atoms: the binding energies of the states in the *p* manifold increase, and the gap between the *p* manifold and the HOMO (of Na character) is still substantial (1.3 eV). The energy-level diagram indicates that Na_7Sn_4 is the last cluster with a well-defined $(Sn_4)^{4-}$ unit. The stabilization of the *p*-like states of the polyanion increases a little, but a level with pure Na character begins to interact strongly with those *p* levels, and this interaction is a precursor of the destabilization of the *p* manifold, which occurs for Na_8Sn_4. The structures in Fig. 2 show that the breakup of a Sn-Sn bond begins precisely in Na_8Sn_4.

The case of the K clusters is striking. The HOMO-LUMO gap in K_4Sn_4 is 1.4 eV, which is smaller than those in Li_4Sn_4 and Na_4Sn_4. Nevertheless, the electronic structure of $(Sn_4)^{4-}$ becomes stabilized by the addition of K atoms. The manifold of polyanion levels stays well separated from the upper levels with K character, and smoothly drops toward the corresponding levels of a pure Sn_4 tetrahedron. Evidently, these levels cannot align with those of the pure Sn_4 because the tetrahedron is charged in the K environment. The reduced interaction between Sn atoms as Sn-Sn bonds are broken apart in the Li_nSn_4 and Na_nSn_4 clusters is reflected in the evolution of the deepest energy levels in Figs. 4 and 5, which approach the binding energy of the 5*s* level of a single Sn atom. In contrast, the K_nSn_4 clusters do not show this behavior because the Sn_4 cluster does not break up.

Also shown in Figs. 4–6 are the Fermi levels E_f of the bcc alkali metals determined from the measured work functions,[32] and the widths of the occupied conduction bands obtained from our calculations using 64 **k** points and an en-

ergy cutoff of 16 Ry. These energies are relevant for the behavior of the clusters for large n when the system amounts to an impurity Sn_4 immersed in a piece of alkali metal. Under these circumstances the set of alkali s levels will have broadened into the metallic conduction band occupied up to the Fermi level. In addition, the energy spectrum will contain levels associated with Sn_4, some of which may be degenerate with, and hybridize with, the alkali conduction band, and consequently will be broadened. The stability of a particular arrangement of the Sn_4 in the metallic environment will depend on the relative occupancy of the bonding and antibonding molecular orbitals. This in turn depends on the position of the Fermi level with respect to the molecular levels, and the degree of broadening of these levels which would result in some bonding levels being promoted above E_f, and some antibonding levels being occupied. Another lesser factor in the stability would be the effects of screening the interactions between the Sn atoms by the metallic electrons. However, a glance at Figs. 5 and 6 shows that even for $n=10$, when the first coordination shell of alkali atoms around the Sn_4 must be nearly full, the clusters are far from the alkali-metal limit. The Na and particularly the K levels lie within a small range of energies, and are not yet spread over the conduction bandwidth. Furthermore, all the alkali atoms are on the surfaces of the clusters. Nevertheless, the stability of the Sn_4 tetrahedron when n is large enough to approach the metallic limit is worthy of study.

From the results of the calculations one can make the following inference concerning the stability of the Sn_4 tetrahedral clusters in the solid and liquid alloys. The reasons for the stability of Sn_4 clusters in the equiatomic solid compounds of Sn with Na, K, Rb and Cs, and their absence in the compound with Li, are the same as for the stability of Pb_4 clusters in the corresponding Pb alloys; these reasons were already discussed in detail elsewhere.[8,13] The equiatomic liquid alloys show some interesting characteristics. According to *ab initio* molecular-dynamics simulations, the Sn_4 clusters survive, after melting, in the liquid equiatomic KSn alloy but not in the liquid NaSn alloy.[9] In our opinion this can be explained by the breaking of Sn-Sn bonds seen in Na_nSn_4 clusters with $n=7$ or larger. When the solid NaSn compound melts, the thermal fluctuations in the liquid will cause some Na dimers to be in contact with the Sn_4 clusters, leading to the breakup of many tetrahedra. In contrast, Figs. 1 and 2 show that the Sn_4 clusters remain as a compact structural unit in a K environment. We next focus on alkali-rich alloys. The high stability of the Sn_4 tetrahedron in K_nSn_4 clusters suggests that Sn_4 clusters could spontaneously form in K-rich liquid alloys. Neither experiments nor theoretical simulations have been performed, to our knowledge, that could test this prediction. Besides the very stable equiatomic compound, the phase diagram of the K-Sn system shows only one K-rich compound and two Sn-rich compounds. We think that the high stability of the Sn_4 tetrahedral cluster itself could be the cause of the paucity of compounds with other than equiatomic composition. The strong tendency of Sn atoms to form Sn_4 tetrahedral clusters in a K environment means that a KSn solid alloy rich in K would consist of Sn_4 clusters surrounded by an excess of K atoms, where only a part of these K atoms is able to transfer the outer electron to the Sn_4 clusters. But a crystalline compound phase does exist in which all the K atoms are able to transfer the valence electron to the Sn_4 clusters, that is, the well-known equiatomic compound. In other words, a hypothetical K-rich alloy containing Sn_4 tetrahedral clusters would decompose into a more stable mixture of crystallites of the equiatomic compound and the pure K metal. The analysis of Figs. 1, 2, and 4–6 indicates that the stability of the Sn_4 tetrahedron will be enhanced in an environment of Rb and Cs. With the arguments given above, it will be most unlikely that the solid compounds rich in Rb or Cs could form. These expectations are supported by the phase diagrams of Sn with Rb and Cs: alkali-rich compounds are not found in these two systems.[10]

IV. CONCLUSIONS

We have investigated the stability of a Sn_4 tetrahedron in alkali atom environments through calculations of A_nSn_4 (A = Li, Na, and K) clusters, starting at $n=4$, and adding alkali atoms one by one to the cluster until $n=10$. We found that the Sn_4 tetrahedron is unstable in Li_nSn_4 clusters, opening into a Sn_4 butterfly at $n=5$, and completely pulled apart at $n=10$. For K_nSn_4 clusters, however, the Sn_4 tetrahedron remains robust for all values of n studied, while Na_nSn_4 clusters are an intermediate case, in which the Sn_4 tetrahedron opens into a butterfly at $n=8$ and appears to break up into two Sn dimers for $n \geqslant 10$. The active species responsible for cutting the Sn-Sn bonds of the Sn_4 tetrahedron in Li_nSn_4 clusters was found to be the Li_2 unit, which, owed to the small size and relatively strong bonding between the Li atoms, acts as a razor blade by slicing into the Sn_4 tetrahedron. Compared with Sn, the K atoms are too large and the bonding between them is far less competitive, and so they cannot even distort the Sn_4 tetrahedron substantially.

Combining with earlier work,[8,9,13] we now have a more complete picture about the stability of Sn_4 Zintl complexes in solid and liquid alkali-tin alloys. The absence of Sn_4 tetrahedra in LiSn alloys is the result of the combination of the following two effects. On the one hand, Li ions are not large enough to properly separate Sn_4 tetrahedra and so the occupied molecular orbitals from different Sn_4 tetrahedra overlap, making the tetrahedra unstable. On the other hand, Li ions are small enough, and the bonding between them is strong enough, that they can squeeze into the tetrahedra and break the Sn-Sn bonds. In the case of KSn alloys, because K ions are large and the bonding between them is weak, the key role they play, besides transferring electrons to Sn atoms, is to separate Sn_4 tetrahedra, which keeps the tetrahedra intact and robust in the alloys. Our results suggest that Sn_4 tetrahedra might survive in K-rich alloys (and also in Rb-rich and Cs-rich alloys), and offer an explanation of why there is a paucity of alkali-rich compounds.

ACKNOWLEDGMENTS

The work was supported jointly by the Natural Sciences and Engineering Research Council of Canada, DGES (Grant No. PB98-0345), and NATO (Grant No. CRG 961128).

[1] P. Jena, S. N. Khanna, and B. K. Rao, Mater. Sci. Forum **232**, 1 (1996).
[2] W. Krätschmer, L. D. Lamb, K. Fostiropoulos, and D. R. Huffman, Nature (London) **347**, 354 (1990).
[3] A. P. Seitsonen, M. J. Puska, M. Alatalo, R. M. Nieminen, V. Milman, and M. C. Payne, Phys. Rev. B **48**, 1981 (1993); C. Ashman, S. N. Khanna, F. Liu, P. Jena, T. Kaplan, and M. Mostoller, *ibid.* **55**, 15 868 (1997).
[4] W. van der Lugt, J. Phys.: Condens. Matter **8**, 6115 (1996); **8**, 8429(E) (1996).
[5] M. Schöne, R. Kaschner, and G. Seifert, J. Phys.: Condens. Matter **7**, L19 (1995); R. Kaschner, M. Schöne, G. Seifert, and G. Pastore, *ibid.* **8**, L653 (1996); G. Seifert, R. Kaschner, M. Schöne, and G. Pastore, *ibid.* **10**, 1175 (1996).
[6] Y. Senda, F. Shimojo, and K. Hoshino, J. Phys.: Condens. Matter **11**, 2199 (1999); **11**, 5387 (1999); **12**, 6101 (2000).
[7] M. Miyata, T. Fujiwara, S. Yamamoto, and T. Hoshi, Phys. Rev. B **60**, R2135 (1999).
[8] L. M. Molina, J. A. Alonso, and M. J. Stott, Solid State Commun. **108**, 519 (1998); J. Chem. Phys. **15**, 7053 (1999).
[9] J. Hafner, K. Seifert-Lorenz, and O. Genser, J. Non-Cryst. Solids **250-252**, 225 (1999); O. Genser and J. Hafner, J. Phys.: Condens. Matter **13**, 959 (2001); **13**, 981 (2001); Phys. Rev. B **63**, 144204 (2001).
[10] T. B. Massalski, H. Okamoto, P. R. Subramanian, and L. Kacprzak, *Binary Alloy Phase Diagrams* (ASM International, Materials Park, OH, 1990).
[11] R. Xu, T. de Jonge, and W. van der Lugt, Phys. Rev. B **45**, 12 788 (1992).
[12] L. M. Molina, M. J. López, J. A. Alonso, and M. J. Stott, Ann. Phys. (Leipzig) **6**, 35 (1997); L. M. Molina, M. J. López, A. Rubio, J. A. Alonso, and M. J. Stott, Int. J. Quantum Chem. **69**, 341 (1998).
[13] J. A. Alonso, L. M. Molina, M. J. López, A. Rubio, and M. J. Stott, Chem. Phys. Lett. **289**, 451 (1998).
[14] H. T. J. Reijers, M.-L. Saboungi, D. L. Price, J. W. Richardson, Jr., K. J. Volin, and W. van der Lugt, Phys. Rev. B **40**, 6018 (1989).
[15] E. Zintl and G. Brauer, Z. Phys. Chem. Abt B **20**, 245 (1933); E. Zintl and G. Wolterdorf, Z. Elektrochem. **41**, 876 (1935).
[16] W. Geertsma, J. Dijkstra, and W. van der Lugt, J. Phys. F **14**, 1883 (1984); W. van der Lugt and W. Geertsma, J. Non-Cryst. Solids **61-62**, 187 (1984); W. Geertsma, J. Phys. C **18**, 2461 (1985).
[17] M. Bockstedte, A. Kley, J. Neugebauer, and M. Scheffler, Comput. Phys. Commun. **107**, 187 (1997).
[18] W. Kohn and L. J. Sham, Phys. Rev. **140**, A1133 (1965).
[19] J. P. Perdew and Alex Zunger, Phys. Rev. B **23**, 5048 (1981).
[20] D. M. Ceperley and B. J. Alder, Phys. Rev. Lett. **45**, 566 (1980).
[21] M. Fuchs and M. Scheffler, Comput. Phys. Commun. **119**, 67 (1999).
[22] L. Kleinman and D. M. Bylander, Phys. Rev. Lett. **48**, 1425 (1982).
[23] S. G. Louie, S. Froyen, and M. L. Cohen, Phys. Rev. B **26**, 1738 (1982).
[24] O. Dieguez and M. J. Stott (unpublished).
[25] C. Majumder, S. K. Kulshreshtha, G. P. Das, and D. G. Kanhere, Chem. Phys. Lett. **311**, 62 (1999).
[26] C. Kittel, *Introduction to Solid State Physics* (John Wiley & Sons, New York, 1986).
[27] K. P. Huber and G. Herzberg, *Constants of Diatomic Molecules* (Van Nostrand Reinhold, New York, 1979).
[28] V. E. Bondybey, M. C. Heaven, and T. A. Miller, J. Chem. Phys. **78**, 3593 (1983).
[29] K. Pak, M. F. Cai, T. P. Dzugan, and V. E. Bondybey, Faraday Discuss. Chem. Soc. **86**, 153 (1988).
[30] B. Wang, L. M. Molina, M. J. López, A. Rubio, J. A. Alonso, and M. J. Stott, Ann. Phys. (Leipzig) **7**, 107 (1998).
[31] B. Wang, M.S. thesis, Queen's University, 1997.
[32] G. W. C. Kaye and T. H. Laby, *Tables of Physical and Chemical Constants* (Longman Group Limited, Harlow, England, 1995), p. 393.